

## GRAPHENE FOR ENVIRONMENTAL AND BIOLOGICAL APPLICATIONS

T. S. SREEPRASAD and T. PRADEEP\*

*DST Unit of Nanoscience, Department of Chemistry,  
Indian Institute of Technology Madras, Chennai – 600036, India*

*\*pradeep@iitm.ac.in*

Received 13 October 2011

Published 16 July 2012

The latest addition to the nanocarbon family, graphene, has been proclaimed to be the material of the century. Its peculiar band structure, extraordinary thermal and electronic conductance and room temperature quantum Hall effect have all been used for various applications in diverse fields ranging from catalysis to electronics. The difficulty to synthesize graphene in bulk quantities was a limiting factor of it being utilized in several fields. Advent of chemical processes and self-assembly approaches for the synthesis of graphene analogues have opened-up new avenues for graphene based materials. The high surface area and rich abundance of functional groups present make chemically synthesized graphene (generally known as graphene oxide (GO) and reduced graphene oxide (RGO) or chemically converted graphene) an attracting candidate in biotechnology and environmental remediation. By functionalizing graphene with specific molecules, the properties of graphene can be tuned to suite applications such as sensing, drug delivery or cellular imaging. Graphene with its high surface area can act as a good adsorbent for pollutant removal. Graphene either alone or in combination with other materials can be used for the degradation or removal of a large variety of contaminants through several methods. In this review some of the relevant efforts undertaken to utilize graphene in biology, sensing and water purification are described. Most recent efforts have been given precedence over older works, although certain specific important examples of the past are also mentioned.

*Keywords:* Graphene oxide; functionalization; sensing; water purification; therapy.

### 1. Introduction

Graphene, the latest addition to the nanocarbon family, is a single atom thick extended two-dimensional (2D) sheet made up of honey comb array of carbon atoms which has become one of the hottest topics in the fields of materials science, physics, chemistry and nanotechnology. It is the building block for other allotropes such as 0D fullerene, 1D carbon nanotubes and 3D graphite. However, graphene has some special properties compared to other forms such as its unusual structural characteristics and electronic flexibility. Properties such as high planar surface area ( $\sim 2630 \text{ m}^2/\text{g}$ ), exceptional electrical ( $\sim 2000 \text{ S/cm}$ ) and thermal

(5300 W/mK) conductivity, transparency to visible light, exceptional mechanical strength (Young's modulus,  $\sim 1100$  GPa) have all been expected to aid in many technological applications. However, most of the reported works in graphene related materials are concerned with catalytic or electronic processes. Two of the emerging areas of application for graphene based materials are in biology and environment.

In this review, the use of graphene (mostly the chemical analogue graphene oxide (GO) and reduced graphene oxide (RGO) and their composites for biology and water purification is outlined. Chemistry has provided many comforts and benefits to mankind. However, now we are facing the great task of cleaning the waste generated during industrial and agricultural activities, which contaminates our air and water. The search for a cheap and highly efficient adsorbent is still on. Due to its large surface area and the abundance of functional groups, graphene seems to be an ideal candidate. The recent research activities emphasize this point. Nanomaterials, due to the similarities to the size regime of biomolecules, have been interesting for applications in biotechnology. However, cytotoxicity of some of the nanomaterials is a major hindering factor when they are considered for specialized applications such as drug delivery or cellular imaging. Chemically prepared graphene, owing to the presence of large functionalities which can be functionalized as per need, put forth a new vehicle for such applications, where the biocompatibility can be modulated by easy functionalization. Hence this review focuses on the application of graphenic materials in biology and environmental remediation/sensing applications. Because of the similarities, the term "graphene" will be used commonly for both GO and RGO in some places. Efforts undertaken to use graphene or its composites for sensing and/or removing contaminants from water will be focused upon. Some application possibilities in biology which can have indirect applications in water purification will also be discussed. Graphene as a nanostructure and its biocompatibility and bio-studies also will be discussed briefly.

### ***1.1. Graphene for environmental applications***

All life forms depend on the availability of pure water. Water gets greatly affected by agricultural and industrial activities. Nanomaterials, owing to their unique properties such as high surface area and greater number of reaction sites per unit area are being considered as potential candidates for removing various contaminants from air and water. A large variety of nanosystems is being considered or is being used for this purpose now. A recent review by Pradeep and Anshup,<sup>1</sup> illustrates the large versatility of nanosystems for these applications. Traditionally, carbon based materials have found to be useful in water purification. Bulk carbon (activated) is a versatile adsorbent that is heavily used to remove various pollutants from the aqueous medium. Carbon in the native form and its composites has been investigated to improve the removal capacity. Recent attention has been focused on carbon based nanomaterials for decontamination and sensing contaminants from water. Nanocarbon forms like carbon nanotubes have been frequently used for this application.

Even though historically the most important and widely used application of bulk carbon is in environmental remediation, the use of graphene or their chemical counterparts, GO and RGO [also known as chemically converted graphene (CCG)] for this applications is limited. Features such as large surface area and presence of surface functional groups can make these systems highly desirable adsorbent candidates. Most applications of graphene have been reviewed. However, the use of graphenic materials for large-scale and down to earth application like water purification is limited. The difficulty in large-scale synthesis was the principal reason behind graphene not being utilized for such applications. The advent of chemical methods and self assembly approaches has assisted to overcome this difficulty. Recent literature has shown that graphene and their composites have been venturing into water purification and sensing.

## 2. Graphene for Sensing Applications: Contaminant and Biological Molecule Sensing

Surface modification or functionalization of graphene surface with specific receptors or functionalities is necessary for exploring sensing applications. A great deal of research activity is happening in this regard. The scope of the review does not allow a detailed description of all the events undertaken. However, a short summary of some of the most relevant efforts is given here.

Most of these efforts are concentrated on developing graphene field-effect transistors (FETs) for chemical and biological sensing. One of the pioneering work on graphene based sensors was done by Schedin *et al.* in 2007, where they detected single gaseous molecules.<sup>2</sup> The step-like changes in resistance caused by the change the local carrier concentration of graphene was used for ultrasensitive detection. Following this, a large number of people have used graphene for sensing. FET devices which are sensitive to hydrogen gas at room temperature were fabricated from RGO with different edge to plane ratios by introducing holes into the basal plane through electrochemical deposition of metal nanoparticles.<sup>3</sup> The change in the electrical conductance of the composite as a function of gas concentration was taken as the sensor response. A mercury detection device was developed by Zhang *et al.* where they self-assembled 1-octadecanethiol monolayers on graphene.<sup>4</sup> These alkanethiol modified graphene FETs were used for mercury detection. The detection of 10 ppm mercury was achieved in this method. Figure 1 shows the atomic force microscope (AFM) and scanning tunnelling microscope (STM) images of the graphene device (Fig. 1(A) and 1(B) respectively). The response of the device to 10 ppm mercury also can be seen [Fig. 1(C)]. Lu *et al.* found that under a positive gate potential ( $V_g$ ), RGO device can give an instantaneous response and fast recovery for  $\text{NH}_3$  sensing at room temperature and the sensing behavior can be modulated by controlling  $V_g$ .<sup>5</sup> The  $V_g$ -dependent  $\text{NH}_3$  sensing of RGO was mentioned to be due to the ambipolar transport of RGO and the  $V_g$ -induced change in the graphene work function. The Coulomb interaction between  $\text{NH}_3$  and the FET might also contribute to these changes.

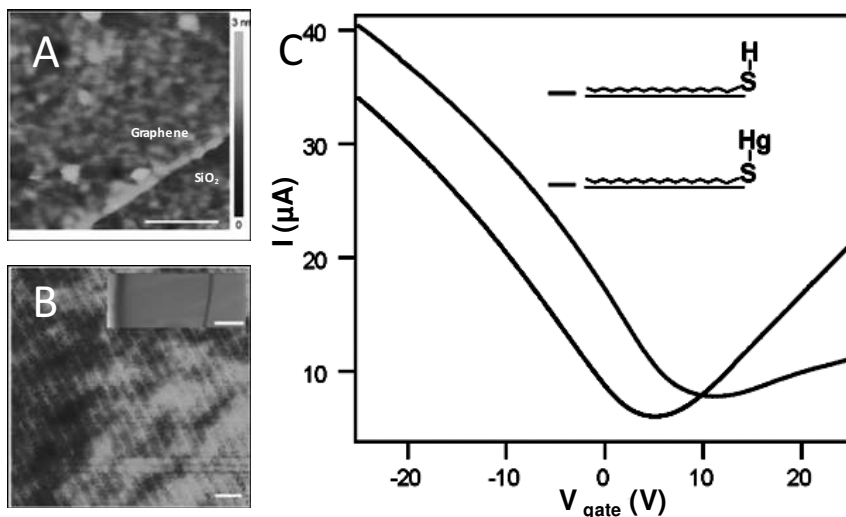


Fig. 1. (A) Tapping-mode AFM showing height and phase images of self-assembled 1-octadecanethiol nanostructures on a single-layer graphene supported on SiO<sub>2</sub> substrate. Scale bars, 100 nm. (B) Large-scale STM image showing configuration details of the self-assembled 1-octadecanethiol on graphene. Scale bar, 10 nm. Inset, optical image of the metal-contacted graphene. Scale bar, 20 μm. (C) Current versus back gate voltage characteristics of a modified graphene FET before (black) and after (red) contacting with 10 ppm mercury solution. Source: Adapted from Zhang *et al.* (2010).

A glucose sensor consisting of graphene platelet-glucose oxidase (GP-GOD) nanostructures, prepared through the self-assembly of GOD and chitosan (CS) functionalized GPs by simple electrostatic attraction between the positively charged CS-stabilized GP and negatively charged GOD was reported by Liu *et al.*<sup>6</sup> The preparation and use of N-doped graphene for glucose bio-sensing with concentrations as low as 0.01 mM in the presence of interferences was reported by Wang *et al.*<sup>7</sup> N-doped graphene was synthesized via nitrogen plasma treatment of graphene synthesized via a chemical method. Also, N-doped graphene electrode showed 400 mV shift in the reduction potential of H<sub>2</sub>O<sub>2</sub> positively with around 20 times current enhancement compared with a glassy carbon electrode.<sup>7</sup> Choi *et al.* reported a flexible conductive composite films made up of GO and nafion through self-assembly and directional convective-assembly in solution chemistry.<sup>8</sup> These films were used for the electrochemical bio-sensing for organophosphate. The system had a sensitivity of 10.7 nA/μM and detection limit of 1.37 × 10<sup>-7</sup> M with a response time of < 3 s.<sup>8</sup> A covalent composite between biocompatible poly-L-lysine (PLL) and graphene nanosheets was used as an amplified biosensor towards H<sub>2</sub>O<sub>2</sub> as well.<sup>9</sup>

A graphene modified electrode for the voltammetric detection of catechol and hydroquinone simultaneously was reported recently.<sup>10</sup> A well-defined peak and significant increase of peak current were observed at the graphene modified glassy carbon electrode (GR/GCE), which clearly demonstrated that graphene could be

used as an efficient promoter to enhance the kinetics of the electrochemical process of catechol and hydroquinone. A composite film consisting of Au nanoparticles and graphene was used for highly selective and sensitive detection of Hg(II).<sup>11</sup> They concluded that the composite film greatly facilitates electron-transfer processes and the sensing behavior for Hg(II) detection, leading to a remarkably improved sensitivity and selectivity. A similar methodology was used for Cd<sup>2+</sup> sensing by Li *et al.*<sup>12</sup> The ultrasensitive platform was fabricated by combining the nafion-graphene nanocomposite film with differential pulse anodic stripping voltameter. They found that using this platform, Cd<sup>2+</sup> can be sensed from real water with good recovery.

Chemically derived GO thin film was used as a humidity sensitive coating on quartz crystal microbalances (QCMs) for humidity detection.<sup>13</sup> The resultant sensors showed excellent humidity sensitivity properties with a maximum sensitivity of 22.1 Hz/% relative humidity (RH) and a linear frequency response versus RH in the wide detection range of 6.4%–93.5% RH. The frequency response of the QCMs was suggested to be dependent on water molecules adsorbed/desorbed masses on GO thin film in the low RH range, and on both water molecules adsorbed/desorbed masses on GO thin film and variations in interlayer expansion stress of GO thin film derived from swelling effect in the high RH range.<sup>13</sup> A highly efficient chemical sensor for ethanol using Al<sub>2</sub>O<sub>3</sub>/Graphene nanocomposites was reported by Jiang *et al.*<sup>14</sup>

Through a facile, one-step process involving supercritical CO<sub>2</sub> (SC CO<sub>2</sub>), Al<sub>2</sub>O<sub>3</sub>/Graphene nanocomposites were fabricated from GO solution. The as-prepared nanocomposite displayed high catalytic chemiluminescence (CL) sensitivity and high selectivity to ethanol gas. An appreciable response was obtained for low concentration of 9.6 mg mL<sup>-1</sup> ethanol at 200°C, pointing the promise of the fabricated nanocomposite. An RGO-quantum dots (QDs) composite for amplified electrochemiluminescence (ECL) based sensing of acetylcholine was reported by Deng *et al.*<sup>15</sup> The structural defects of GO quenches the ECL emission of QDs coated on GO modified electrode. Due to the restoration of double bonds, RGO-QDs showed ECL emission. Two ECL biosensors for choline and acetylcholine were fabricated by covalently cross-linking choline oxidase (ChO) or ChO-acetylcholinesterase on the QDs/RGO modified electrode. This showed the linear response ranges and detection limits of 10–210 μM and 8.8 μM for choline, and 10–250 μM and 4.7 μM for acetylcholine, respectively.

Another category of sensors based on graphene utilizes Surface-enhanced Raman spectroscopy (SERS) based sensing/detection protocols. Liu *et al.* recently devised an ultrasensitive SERS based strategy for the detection of aromatic molecules.<sup>16</sup> They fabricated Ag nanoparticle attached graphene films where GO acts as the matrix which catches the aromatic molecule and Ag nanoparticles aids in the localized surface plasmon resonance based SERS property. By using positively charged crystal violet (CV), negatively charged amaranth (a cosmopolitan genus of herbs) and neutral phosphorus triphenyl (PPh<sub>3</sub>) as model molecules, they demonstrated the utility of the above hybrid system. A similar strategy for the detection of

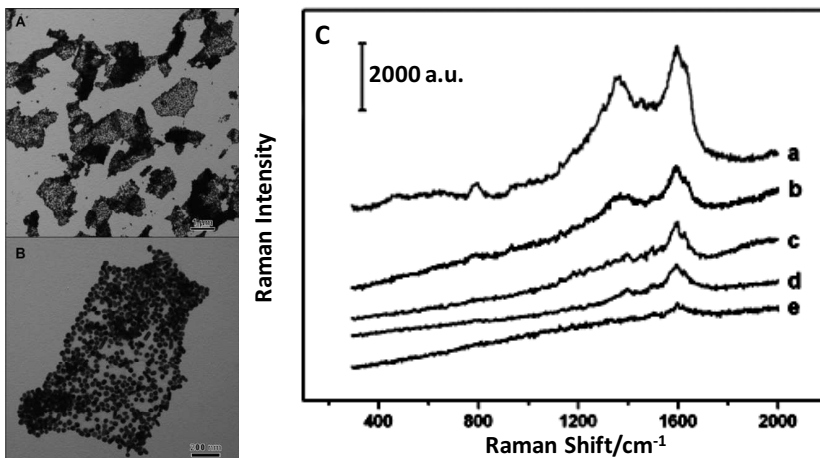


Fig. 2. (A) and (B) TEM images of the GO/PDDA/AgNPs at different magnifications. (C) SERS spectra of 9 nM folic acid obtained in the GO/PDDA/AgNP solutions with (a) 0.02 mg/mL, (b) 0.01 mg/mL, (c) 0.004 mg/mL, (d) 0.0025 mg/mL, (e) 0.002 mg/mL graphitic carbon. Source: Adapted from Ren *et al.* (2011).

folic acid was also reported recently. Through a self-assembly method with the help of poly(diallyldimethyl ammonium chloride) (PDDA) as the functional macromolecules, GO/Ag nanoparticle hybrids (GO/PDDA/AgNPs) were fabricated. Using the SERS enhancement of the hybrid, folic acid was detected with a very low detection limit of 9 nM. Figure 2 shows the TEM images (A and B) and the SERS detection capability of the formed composite.

Graphene has been used for biosensing applications as well. Li *et al.* developed a graphene-based fluorescence resonance energy transfer (FRET) biosensor which included a fluorescein amidite (FAM)-labeled ssDNA adsorbed onto GO.<sup>17,18</sup> The FRET between FAM and GO, results in the rapid quenching of luminescence. However, the binding between probe ssDNA and a complementary ssDNA changes the conformation, and releases FAM-ssDNA from the GO surface, restoring fluorescence which results in the detection. Mohanty and Berry reported a graphene based bio-device which can sense single bacterium and can work as a label-free DNA sensor.<sup>19</sup> The attachment of single-bacterium generated  $\sim 1400$  charge carriers in a *p*-type chemically modified graphene and single-stranded DNA tethered on graphene hybridizes with its complementary DNA strand, increased the hole density by  $5.61 \times 10^{12} \text{ cm}^{-2}$ . Figure 3 illustrates the usefulness and accuracy of the FETs fabricated. Ohno *et al.* recently reported a graphene based FET for chemical and biological sensing application.<sup>20</sup> Single layer graphene obtained from micromechanical cleavage was used to construct FET, which can sense change in solution pH with a lowest detection limit (signal/noise = 3) of the 0.025. Using the same set up they were able to detect different charge types of biomolecules due to their isoelectric point. Jang *et al.* developed a graphene-based FRET platform that has

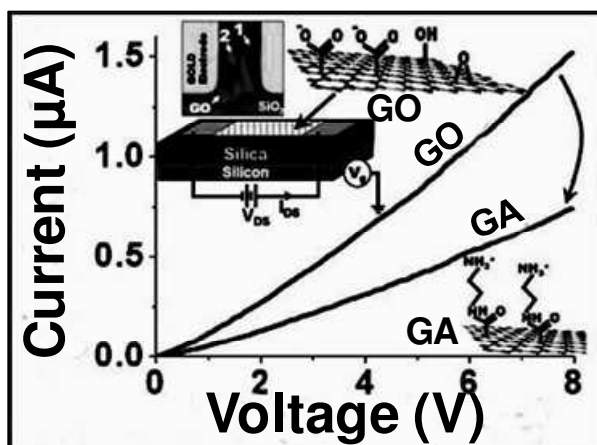


Fig. 3. Current-voltage behavior of the GO and GA devices. The insets show the device with GO/GA between gold electrodes and a schematic of the GO and GA's chemical structure. Source: Mohanty and Berry (2008).

been developed for detection of helicase-mediated unwinding of duplex DNA.<sup>21</sup> Graphene-based FRET biosensors for multicolor DNA analysis was developed by He *et al.*<sup>22</sup> Employing molecular beacons (MBs), graphene-based FRET biosensors were fabricated with enhanced sequence-specific detection of target DNA.<sup>23</sup> The two ends of a MB were labeled with a fluorophore and a GO/RGO. MBs did not fluoresce until they have hybridized with the target. In this study, quantum dots were used as the fluorophores owing to its broad absorption and narrow emission spectra. This FRET biosensor displayed good selectivity and high sensitivity, with a detection limit for target cyclin DNA of 12 nM.<sup>23</sup> GO has been used as the 'nanoquencher', with increased sensitivity and single-base mismatch selectivity for target DNA as well.<sup>24</sup> Choi *et al.* recently devised a strategy to develop a electrical sensor for DNA.<sup>25</sup> Through microwave-assisted sulfonation, highly water-soluble graphene sheets were synthesized and the complex interactions of the functionalized graphene with DNA resulted in an advanced resistive sensing platform for the electrical detection of label-free DNA.

Graphene based FET have been developed for the sensing of ion, small molecules and proteins as well. Most of these studies utilized the specific binding of aptamers towards target molecules. Wen *et al.* devised a graphene based FET containing Ag<sup>+</sup>-specific aptamer for the detection of Ag<sup>+</sup>.<sup>26</sup> Ag<sup>+</sup> induces a conformational change of the aptamer which in turn leads to the recovery of FAM fluorescence. A highly selective FRET sensor for detection of bovine thrombin was developed by Chang *et al.*<sup>27</sup>

The detection procedure was similar to earlier report. However, a dye-labeled aptamer probe and graphene was used in this study. Sodium dodecyl benzene sulfonate (SDBS) was used for the chemical reduction of GO to produce SDBS-graphene.

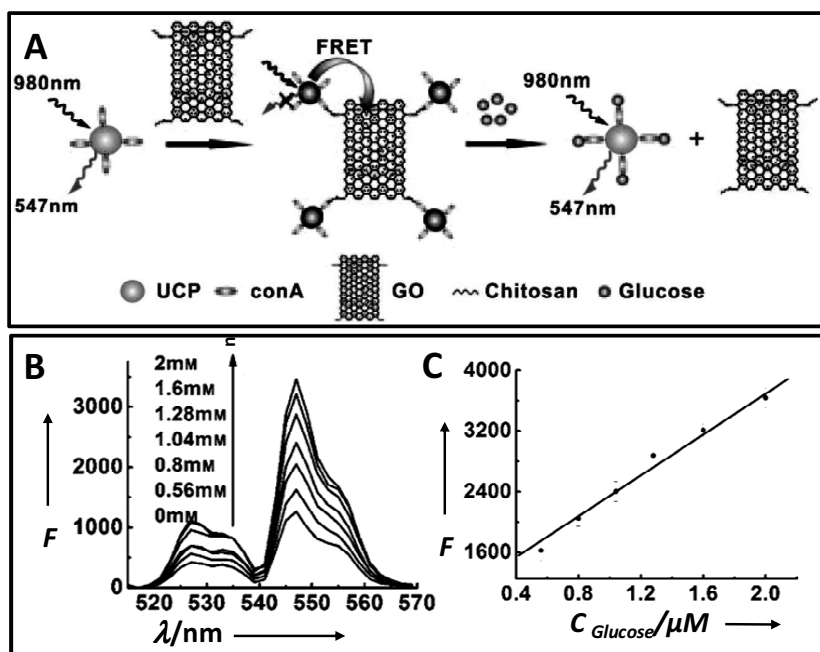


Fig. 4. (A) Schematic illustration of the UCP–GO biosensing platform and the mechanism of glucose determination. (B) Fluorescence emission spectra of GO–CS–ConA–UCP complex in the presence of different concentrations of glucose in diluted serum. (C) Linear relationship between donor fluorescence intensity and glucose concentrations. *Source:* Adapted from Zhang *et al.* (2011).

Thrombin aptamer labeled with FAM was incubated with SDBS–graphene and upon introduction of thrombin into the aptamer/graphene solution, fluorescence recovery was observed. This was used for the detection. This graphene-based FRET sensor had a sensitive detection limit for thrombin in buffer upto 31.3 pM.

Change in fluorescence has been utilized for sensing of many materials. Recently graphene based sensors utilizing the change in fluorescence have appeared. A novel sensor for glucose determination based on FRET from upconverting phosphors (UCP) to GO was devised by Zhang *et al.*<sup>28</sup> The FRET from anti-Stokes fluorophores like UCP to GO was utilized for detecting glucose directly in serum samples. They also extended the strategy for the detection of other biologically significant molecules. Figure 4 illustrates the mechanism of sensing. Xu *et al.* reported a graphene based platform for the recognition of bovine serum albumin (BSA).<sup>29</sup> They found that the binding of squaraine (SQ) dyes to RGO/GO would enhance the fluorescence response of SQ to BSA. The attachment of SQ dyes to GO surface resulted in the quenching of its fluorescence and when BSA interacts with this hybrid resulted in the triggering of large fluorescence and hence the recognition of BSA. A novel GO based fluorescent biosensor platform for the sequence-specific recognition of double-stranded DNA (dsDNA) was formulated by Wu *et al.* recently which is based upon the DNA hybridization between dye-labeled single-stranded

DNA (ssDNA) and double-stranded DNA.<sup>30</sup> FAM labeled ssDNA upon adsorption onto GO loses its fluorescence. When the target dsDNA is added, hybridization occurs between this and ssDNA by desorbing it from GO. This results in the turning on of the fluorescence of the dye. The detection limit was found to be 14.3 nM in this method.

Using a similar strategy, an intracellular protease sensor for capsase-3 was reported by Wang *et al.*<sup>31</sup> Fluorescence based strategy has been extended to metal ion sensing as well. A RGO–organic dye nanoswitch for the label-free, inexpensive, sensitive and selective detection of  $\text{Hg}^{2+}$  was recently reported by Huang *et al.*<sup>32</sup> Here, RGO functions as an effective nanoquencher and highly selective nanosorbent. Acridine orange (AO) dye was anchored onto RGO via  $\pi$ -stacking interactions which resulted in the effectively quenching the fluorescence of AO because of the occurrence of long range resonance energy transfer (LrRET). When  $\text{Hg}^{2+}$  selectively gets attached to RGO, the interaction between the dye and RGO will be disturbed, resulting in restoration of dye fluorescence. The detection limit for  $\text{Hg}^{2+}$  was estimated to be about 2.8 nM. Graphene-DNAzyme based biosensor for amplified fluorescence “Turn-On” detection of  $\text{Pb}^{2+}$  was also reported recently. The detection limit of the devise was found to be 300 pM.<sup>33</sup>

### 3. Graphene for Water Purification Related Applications

Historically, one of the major application arenas of carbon based materials has been in water purification. Carbon based materials ranging from charcoal to activated carbon to graphite have all been used for this purpose. The emergence of carbon based nanomaterials such as carbon nanotube (either pristine or as composite) has also been used for decontamination of drinking water. Recent literature suggests that the 2D graphene (RGO/GO) is also getting into this application. Due to the high surface area this material possesses, most of these efforts have been concentrated in using this exceptional surface area and to use RGO/GO as an adsorbent. Some relevant work in this regard is summarized here. Some efforts to construct composite useful for catalytic decomposition of contaminants are described first.

Photo-catalytic decomposition of contaminants using nanomaterials has seen intense research activity in recent times. Graphene based composites showed considerable efficiency in this aspect. The photocatalytic degradation of dye over a graphene gold nanoparticle hybrid under visible light irradiation was proposed by Xiong *et al.* for the first time.<sup>34</sup> Gold nanoparticles were deposited on the graphene substrate by the spontaneous reduction of  $\text{HAuCl}_4$  by RGO. The photoactivity of RGO–Au was evaluated using rhodamine B (RhB) under visible light irradiation. A mechanism was proposed for the degradation as well. The dye will first get excited to dye\*, which is followed by an electron transfer from dye\* to graphene. Then, the electron is moved to a gold nanoparticle and will be trapped by  $\text{O}_2$  to produce various reactive oxidative species (ROSSs). The dye<sup>+</sup> finally degrades either by itself and/or by the ROSSs. Zhu *et al.* reported a graphene enwrapped

Ag/AgX (X = Br, Cl) nanocomposite plasmonic photocatalyst at water/oil interface.<sup>35</sup> They used it as a stable plasmonic photocatalyst for the photodegradation of methyl orange (MO) under visible-light irradiation. The combination of Ag/AgX with GO nanosheets resulted in the increased adsorptive capacity of Ag/AgX/GO to MO molecules whereas the smaller size of the Ag/AgX nanoparticles in Ag/AgX/GO, facilitated charge transfer, and the suppressed recombination of electron-hole pairs in Ag/AgX/GO resulting in the enhanced photocatalytic activity. Graphene-semiconductor composite has also been used for decontamination of water. GO-TiO<sub>2</sub> composite have been regarded widely as the best photocatalyst. Akhavan *et al.* synthesized GO nanosheets on TiO<sub>2</sub> thin films and used them for the photoinactivation of bacteria (*E. coli*) under solar illumination.<sup>36</sup> The incorporation of GO onto TiO<sub>2</sub> increased the antibacterial activity by a factor of 7.5. A composite prepared by self-assembling TiO<sub>2</sub> nanorods on large area GO sheets at a water/toluene interface was used for the photocatalytic degradation of methylene blue (MB) under UV light irradiation.<sup>37</sup> The large enhancement of photocatalytic activity was concluded to be due to the effective charge anti-recombination and the effective absorption of MB on GO. It was also observed that the degradation rate of MB in the second cycle is faster than that in the first cycle because of the reduction of GO under UV light irradiation.

Using TiCl<sub>3</sub> and GO as reactants, a GO-TiO<sub>2</sub> composites were fabricated by Chen *et al.*<sup>38</sup> The composite could be excited by visible light of wavelength higher than 510 nm. The composite was found to be useful in visible light induced degradation of MO. A TiO<sub>2</sub>-graphene composite for the photodegradation of volatile organic solvent in the gas phase was reported by Zhang *et al.*<sup>39</sup> A TiO<sub>2</sub>-graphene composite was prepared using hydrothermal reaction of GO and TiO<sub>2</sub> in an ethanol-water solvent. The composite showed much higher photocatalytic activity and stability than bare TiO<sub>2</sub> toward the gas-phase degradation of benzene. Structure and photocatalytic properties of TiO<sub>2</sub>-GO intercalated composite was reported by Zang *et al.*<sup>40</sup> The composite was successfully prepared at 80°C with GO and titanium sulfate (Ti(SO<sub>4</sub>)<sub>2</sub>) as initial reactants. The photocatalytic properties of the composite under UV light showed that the degradation rate of MO is 1.16 mg min<sup>-1</sup> g<sup>-1</sup>. A similar composite was fabricated by the *in situ* growth of TiO<sub>2</sub> in inter-layers of expanded graphite.<sup>41</sup> The composite was used for the photocatalytic degradation of phenol under visible and UV light. The enhanced photocatalytic performance of the composite was concluded to be due to increased charge separation, improved light absorbance and light absorption width, and high adsorptivity for pollutants.

Zhang *et al.* showed that chemically bonded TiO<sub>2</sub> (P25) can be anchored onto graphene surface via a hydrothermal process and can be used for the photocatalytic degradation of dyes.<sup>42</sup> Liang *et al.* synthesized graphene/TiO<sub>2</sub> nanocrystals hybrid by directly growing TiO<sub>2</sub> nanoparticles on GO sheets by a two-step method.<sup>43</sup> First, TiO<sub>2</sub> was first coated on GO sheets by hydrolysis and then crystallized into anatase nanocrystals by hydrothermal treatment in the second step. The composite showed

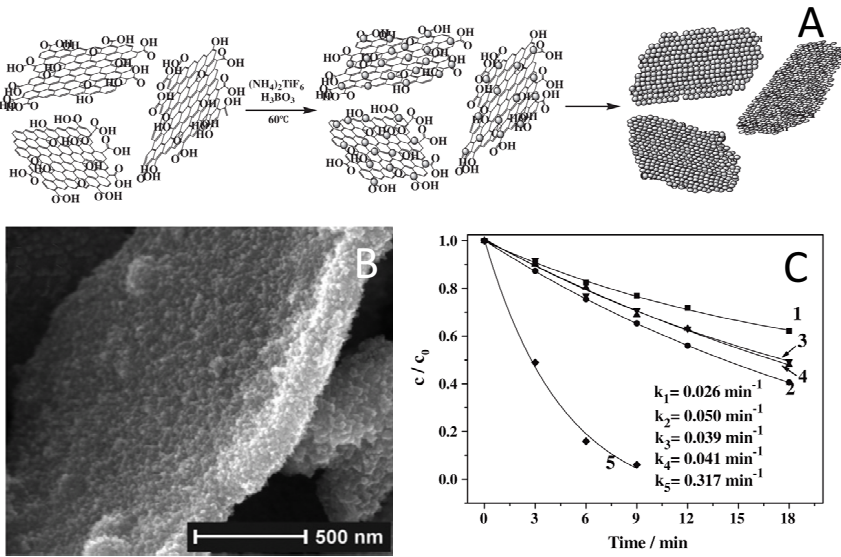


Fig. 5. (A) Schematic illustration of the assembling growth of  $TiO_2$  nanoparticle on graphene oxide sheets. SEM image of (B) heat-treated graphene oxide/ $TiO_2$  composites. (C) Photocatalytic degradation of  $10 \text{ mg L}^{-1}$  methyl orange at pH 4.0 by (1) neat  $TiO_2$ , (2) mixture of neat  $TiO_2$  and graphene oxide, (3) P25, (4) mixture of P25 with graphene oxide, and (5) the heat-treated composite of graphene oxide/ $TiO_2$ . The load of catalyst was  $0.5 \text{ g L}^{-1}$ . *Source:* Adapted from Jiang *et al.* (2011).

threefold enhancement of photocatalytic degradation efficiency over conventional  $TiO_2$  such as P25. Figure 5 illustrate the formation of composite and its photodegradation capacity. Following this, a highly efficient photocatalyst was fabricated by *in situ* deposition of  $TiO_2$  nanoparticles on GO nanosheets by a liquid phase deposition, followed by a calcination at  $200^\circ C$  recently.<sup>44</sup> The composite was utilized for the photocatalytic removal of pollutants. At optimum conditions of solution pH, post-calcination, and at a definite GO content, the photo-oxidative degradation rate of MO and the photo-reductive conversion rate of Cr(VI) over the composites were as high as 7.4 and 5.4 times that over P25. A photocatalyst prepared by anchoring  $TiO_2$  nanoparticles on graphene sheets by sonochemical synthesis was used for the photocatalytic degradation of MB.<sup>45</sup> They found that the photocatalytic activity of the resultant graphene- $TiO_2$  composites containing 25 wt.%  $TiO_2$  is better than that of commercial pure  $TiO_2$ .

The role of GO/RGO content on the photocatalytic efficiency was investigated by Nguyen-Phan *et al.*<sup>46</sup> They prepared  $TiO_2$ /GO composites using a simple colloidal blending method and found that the composites have superior adsorption and photocatalysis performance under both UV and visible radiation compared to pure  $TiO_2$ . They observed that gradually increasing the content of GO up to 10 wt% resulted in the increased removal efficiency and the photodegradation rate of MB.

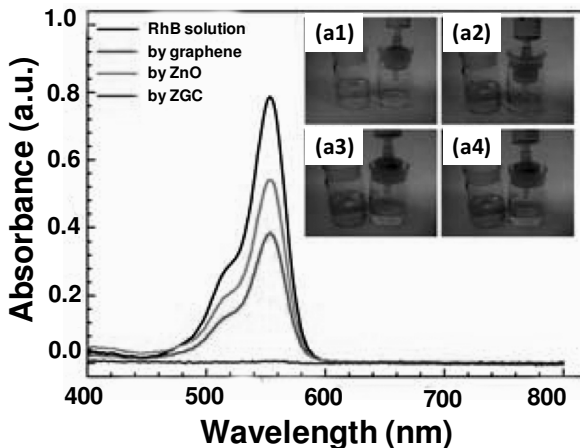


Fig. 6. The UV-visible spectra and images of (a) the original and filtered RhB solutions with graphene (inset a1), commercial ZnO (inset a2), and the ZGC (ZnO graphene composite) (insets a3 and a4). Source: Li and Cao. (2011).

The increase was attributed to synergy effects including the increase in specific surface area with GO amount as well as the formation of both  $\pi$ - $\pi$  conjugations between dye molecules and aromatic rings and the ionic interactions between methylene blue and oxygen-containing functional groups at the edges or on the surfaces of carbon-based nanosheets. They also concluded that here, GO is working as the adsorbent, electron acceptor and photosensitizer to enhance the dye photodecomposition. Graphene-ZnO composites have also been fabricated for the photocatalytic degradation. Li and Cao recently reported a ZnO-Graphene composite which work efficiently as a photocatalyst for the degradation and filtered removal of rhodamine B (RhB).<sup>47</sup> Figure 6 shows the UV vis spectra and photographs of the degradation process. A graphene-MnOOH composite was prepared by solvothermal method recently.<sup>48</sup> The mechanism of composite formation was suggested to be dissolution-crystallization and oriented attachment. The composite showed unusual catalytic performance for the thermal decomposition of ammonium perchlorate (AP) due to the concerted effects of graphene and MnOOH. A graphene-horseradish peroxidase (HRP) composite for catalytic degradation of phenolic compounds was reported by Zhang *et al.*<sup>49</sup>

Microbial contamination is major problem in drinking water. Graphene based solutions for this problem also has been made reported in the literature. An antibacterial brilliant blue (a common colorant)/RGO/tetradecyltriphenylphosphonium bromide composite which is highly dispersible in water and having specific targeting capability was reported by Cai *et al.*<sup>50</sup> The composite was found to be effective against both Gram-positive and Gram-negative bacteria. Figure 7 illustrates the antibacterial activity of the above composites. A silver-GO composite having a superior antibacterial activity towards *E. coli* due to the synergistic effect of GO and

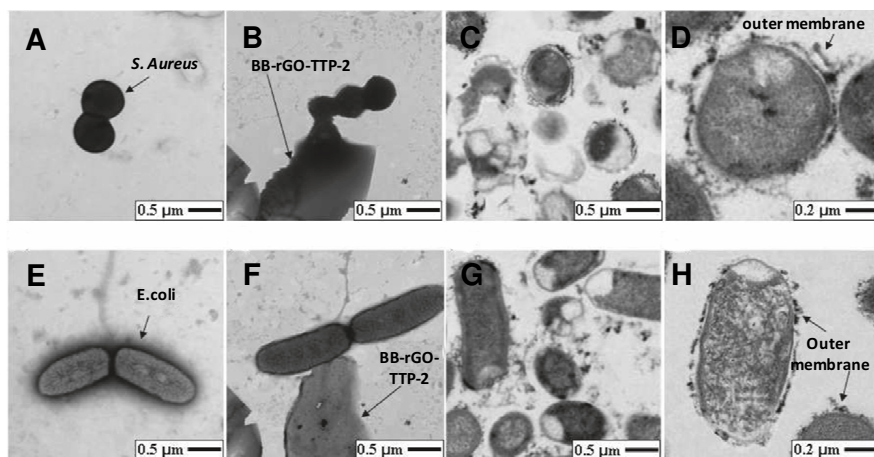


Fig. 7. (A) TEM images of normal *S. aureus* cells (A), *E. coli* cells (E), *S. aureus* cells (B), *E. coli* cells (F) treated by BB-rGO-TTP-2, the changes of *S. aureus* cells (C, D) and *E. coli* cells outer membrane (G, H). Source: Cai. (2011).

silver nanoparticles has been reported.<sup>51</sup> A similar silver based graphene composite which can act as a bactericidal agent for water disinfection was reported by Bao *et al.*<sup>52</sup> A similar monodispersed Ag nanoparticle-graphene composite having enhanced antibacterial property was reported by Liu *et al.* as well.<sup>53</sup>

Utilizing the rich abundance of functional groups, a graphene based composite consisting of an antibacterial bio-polymer chitosan and a bactericidal protein was fabricated recently. The synergetic effect of different materials incorporated resulted in a highly antibacterial composite.<sup>54</sup> The composite showed a tendency to form self-standing films which can aid in coating this composite onto suitable substrates. The formed films can be easily imprinted with different patterns by applying compressive pressures. This pattern can be erased easily after use by simply wetting the film and new pattern can be inscribed. This points to the utility of the films in high end applications such as secure data transfer. Figure 8 illustrates the different aspects of the composite described above.

Capacitive deionization or electrosorption with porous electrodes are thought to be ideal candidates to remove various ions from aqueous solutions. Due to their good conductivity, high surface area and suitable pore size distribution, carbon based materials including activated carbon, carbon fibers, carbon aerogels and carbon nanotubes are employed as electrosorptive electrodes. Graphene also has emerged as an interesting candidate for this application. First attempt in this direction was done by Li *et al.*<sup>55</sup> They synthesized graphene through chemical methods and used as electrosorptive electrodes for capacitive deionization. Electrosorption experiments were conducted in NaCl solutions at low voltage ( $\leq 2$  V) to investigate the electrosorption performance. Graphene exhibited a high electrosorption capacity of 1.85 mg/g where the electrosorption of NaCl onto graphene electrodes is driven by a

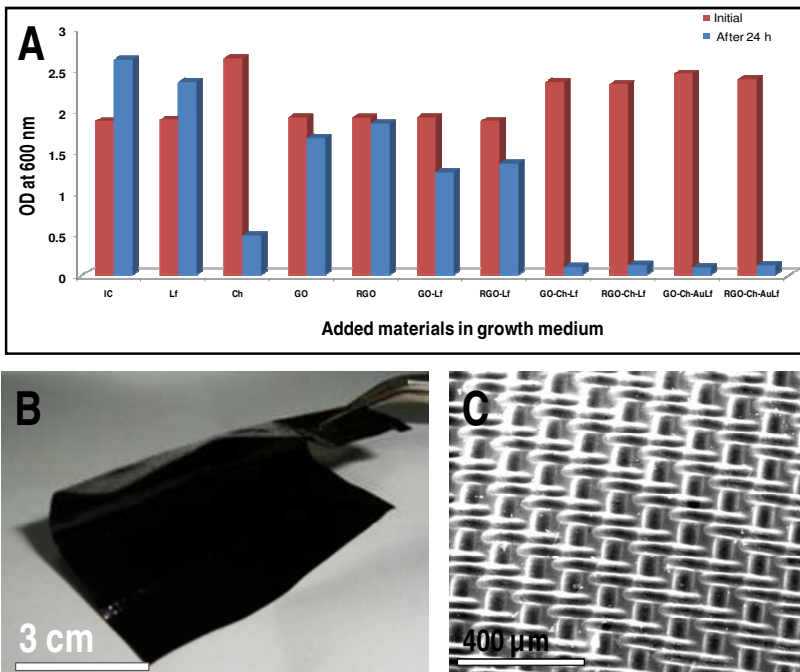


Fig. 8. (A) The plot depicting the antibacterial activity of the composites and the ingredients, (B) the photograph of the formed film and (C) SEM image of pattern imprinted on the film. Source: Sreeprasad *et al.* (2011).

physisorption process. Graphene nano-flakes (GNFs) were used as electrodes to remove ferric ions by capacitive deionization.<sup>56</sup> The optimum flow rate and electrical voltage were 25 ml/min and 2.0 V, respectively and the maximum equilibrium electrosorption capacity and rate constant for FeCl<sub>3</sub> at 2.0 V were 0.88 mg/g and 0.27 min<sup>-1</sup>. The sorption experiment was repeated for different ions to quantify the selectivity and the electrosorption capacities of cations on the GNFs followed the order of Fe<sup>3+</sup> > Ca<sup>2+</sup> > Mg<sup>2+</sup> > Na<sup>+</sup>.

The electrosorptive capacities of GNFs were found to be higher than activated carbon. Electrosorptive performance of GNFs electrodes with different bias potentials, flow rates and ionic strengths were measured and the electrosorption isotherm and kinetics were investigated by Li *et al.*<sup>57</sup> The specific electrosorptive capacity of the GNFs was 23.18 μmol/g for Na<sup>+</sup> at an initial concentration of 25 mg/L, higher than activated carbon under the same experimental conditions. Figure 9 shows the schematics of graphene based capacitive deionization set up [Fig. 9(a) and 9(b)]. The utility of such a device for contaminant removal can also be seen [Fig. 9(c)]. A comparative study of electrosorptive capacities of single wall carbon nanotubes and graphene was also reported recently.<sup>58</sup>

Graphene has recently received attention as a potentially selective material for membranes. Experimental studies and related simulations suggested the feasibility

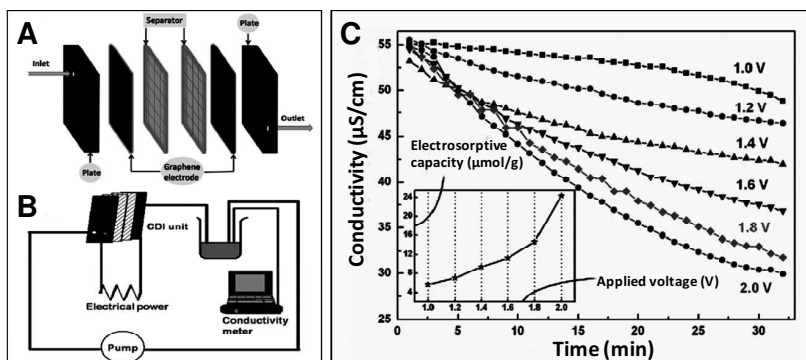


Fig. 9. (A) Schematic of electro-sorptive unit (B) cell batch-mode experiment. The CDI unit consisted of graphite plate, GNFs film, and separator. (C) The electro-sorption of  $\text{Na}^+$  onto GNFs electrode at different bias potentials. *Source:* Adapted from Li. (2010).

of generating subnanometer pores in a controllable fashion on graphene by methods such as electron beam irradiation,<sup>59</sup> ion bombardment<sup>60,61</sup> or by doping.<sup>62</sup> The transport of ions through  $\sim 0.5$  nm pores in graphene terminated with nitrogen or hydrogen was studied using MD simulations.<sup>63</sup> It was understood that the N-terminated pore allow the passage of metal ions such as  $\text{Li}^+$ ,  $\text{Na}^+$ , and  $\text{K}^+$ , while the H-terminated pore allowed  $\text{Cl}^-$  and  $\text{Br}^-$  to pass through, but not  $\text{F}^-$ . The smaller ions had the lowest passage rates due to their strongly bound hydration shells. Suk and Aluru investigated water transport through ultrathin graphene and the rate at which water molecules transport across 0.75–2.75 nm diameter pores in graphene membranes. They also compared it with 2–10 nm long carbon nanotubes (CNTs) with similar diameters. They observed that the flux through graphene pores to be a factor of two of that through CNTs and experiences a significant resistance to transport. Though the studies mentioned above pointed towards the potential of graphene membranes for water desalination with fluxes up to an order of magnitude higher than polymeric RO membranes, experimental measurements of water transport and salt rejection through them are still not realized.

Adsorption, among other technologies for removing pollutants, has proved to be most effective in removing pollutants from dilute solutions. As discussed earlier, carbon in its various forms, including composites, has been traditionally used for this application.<sup>64–66</sup> However, use of graphene was not common for this application until recently. The recent research points that graphene is also highly useful as a high performance adsorbent. Graphene and the composites have proved to be an ideal candidate for the adsorption-based remediation of waste water. The adsorption of thiophene on Single-wall Nanotubes (SWNT) and graphene was investigated theoretically employing periodic boundary conditions and the van der Waals density functional (VDW-DF) and local density approximation (LDA) methodologies by Denis and Iribarne.<sup>67</sup> They suggested that thiophene adopts a nearly parallel configuration with respect to the graphene plane with sulfur atom 3.7 Å above

the sheet, whereas the two hydrogen atoms on carbon atoms not bonded to sulfur are 3.45 Å above it. The adsorption energy for this configuration of thiophene on graphene was calculated to be 8.9 kcal/mol. They investigated some other possible orientations and adsorption energies as well. The use of functionalized graphene prepared via fast method of electrolysis with potassium hexafluorophosphate solution as electrolyte under the static potential of 15 V was used for the adsorption of Pb(II) and Cd(II) by Deng *et al.*<sup>68</sup> The synthesized graphene sheets were having 30 wt.% PF<sub>6</sub><sup>-</sup>. These graphene sheets had adsorption capacities in the order of 406.6 mg/g (pH = 5.1) for Pb(II) and 73.42 mg/g (pH = 6.2) for Cd(II). A GO based solution for removing Cu<sup>2+</sup> was developed by Yang *et al.*<sup>69</sup> They found that aggregation of GO can be induced by Cu<sup>2+</sup> in aqueous solution with a huge Cu<sup>2+</sup> absorption capacity. GO was found to be having 10 times absorption capacity over activated carbon. Liu *et al.* recently developed a strategy to immobilize GO and RGO on silica through covalent binding for the use of these material for solid-phase extraction (SPE).<sup>70</sup> The carboxy groups of GO were linked to the amino groups of an amino-terminated silica adsorbent and upon hydrazine treatment, they obtained RGO@silica.

They used these adsorbents for the removal of chlorophenols. The strategy to immobilize GO/RGO on silica is illustrated in Fig. 10(I). AFM and SEM images are also given [Fig. 10(II)]. Plot depicting the removal efficiency of the adsorbent is also given [Fig. 10(III)]. Graphene can also be produced from various sources such as high molecular petroleum fractions like asphalt or from natural sugars as well. An *in situ* strategy to synthesize and immobilize graphenic materials onto silica substrates was devised by Sreeprasad *et al.* Here, a high efficiency graphenic adsorbent was fabricated on sand particles starting from asphalt. The synthesized adsorbent was highly effective for the adsorption of dyes and pesticides from water. The material was reusable for several cycles.<sup>71</sup> Figure 11 shows the scanning electron microscope (SEM) and energy-dispersive X-ray spectroscopy (EDX) characterization of the adsorbent. The time dependent removal a dye by the adsorbent can also be seen.

Ramesha *et al.* reported the use of GO and RGO for the removal of anionic and cationic dyes such as methylene blue, methyl violet, rhodamine B and orange G from aqueous solutions.<sup>72</sup> For GO, because of the rich abundance of negatively charged functionalities, effective adsorption of cationic dyes took place while the adsorption was negligible for anionic dyes. However, RGO having high surface area is found to be very good adsorbent for anionic dyes. The removal of methylene blue by GO was studied in detail by Yang *et al.*<sup>73</sup> Absorption capacity as high as 714 mg/g was observed. For initial MB concentrations lower than 250 mg/L, the removal efficiency higher than 99% was attained and the solution turned completely colorless. Efficient adsorption of methylene blue dye from an aqueous solution by GO was studied by Zhang *et al.* as well.<sup>74</sup> Zhao *et al.* recently proposed the utility of sulfonated graphene for the management of aromatic pollutants taking naphthalene and 1-naphthol as model pollutants.<sup>75</sup> An adsorption capacity as high

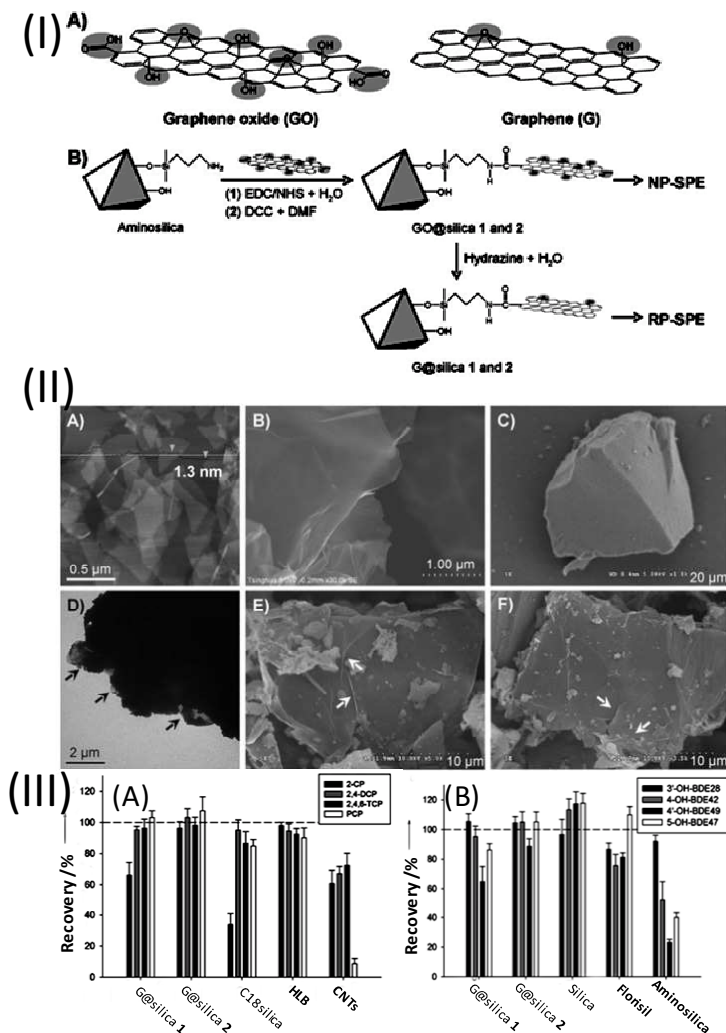


Fig. 10. (I) Chemical routes to the synthesis of GO@silica and RGO@silica. NP-SPE=normal-phase SPE, RP-SPE=reversed-phase SPE. (II) (A) AFM image of GO sheets (B) High-resolution SEM image of GO sheets. (C) SEM image of a bare silica particle. (D) TEM image of a GO@silica particle. E,F) SEM images of GO@silica 1 (E) and RGO@silica 1 (F). (III) Comparison of the analytical performance of G@silica with other adsorbents for the RP-SPE of chlorophenols (A) and GO@silica with other adsorbents for the NP-SPE (B). *Source:* Adapted from Liu *et al.* (2011).

as  $\sim 2.3\text{--}2.4 \text{ mmol g}^{-1}$  for naphthalene and 1-naphthol was observed. The use of graphene as an adsorbent for fluoride from aqueous solution was demonstrated by Li *et al.*<sup>76</sup> Thermodynamic studies indicated that the process was spontaneous and endothermic in nature. Adsorption capacities and rates of fluoride onto graphene at different initial pH, contact time and temperature were also investigated and results revealed that the maximum adsorption capacity is up to 17.65 mg/g at

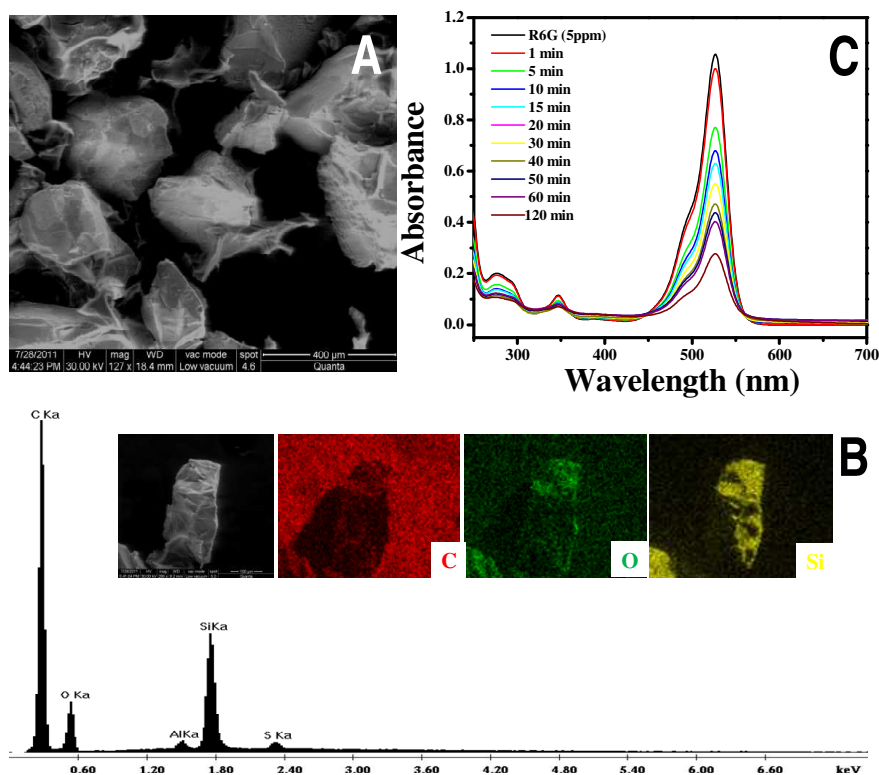


Fig. 11. (A) SEM image of the prepared adsorbent material, (B) EDAX spectrum and elemental maps and (C) Time dependent UV/Vis spectra showing the removal of rhodamine 6G. Source: Sreepasad *et al.* (2011).

initial fluoride concentration of 25 mg/L at 298 K. Graphene sheets prepared by hydrogen induced exfoliation of graphitic oxide followed by functionalization was found to be highly efficient adsorbent system for arsenic and sodium from aqueous solutions.<sup>77</sup> Maximum adsorption capacities for arsenate, arsenite and sodium were calculated to be 142, 139 and 122 mg/g, respectively. Recently Maliyekkal *et al.* found that RGO can function as an efficient adsorbent for pesticides.<sup>78</sup> The adsorption capacities of (CP), endosulfan (ES) and malathion (ML) were as high as ~1200, 1100 and 800 mg/g, respectively. RGO showed 10–20% higher affinity compared to GO, indicating that increasing surface oxygen functionality reduces the affinity of graphenic surface to pesticides. Theoretical calculations indicated that, the adsorption is dependent on the presence or absence of water molecules.<sup>78</sup> Figure 12 depicts the adsorbing ability of RGO towards pesticides.

Generally composites exhibit enhanced properties compared to the ingredients. A variety of graphene composites have been reported for the remediation of polluted water. One of the first attempt in this direction was from Chandra *et al.* who made water-dispersible magnetite-RGO composite and used it for arsenic removal.<sup>79</sup> The

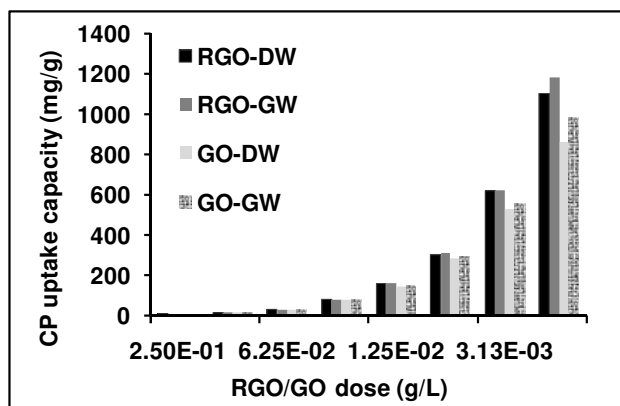


Fig. 12. Plot depicting the variation in CP uptake capacity of GO/RGO with varying dose. Source: Maliyekkal *et al.* (Unpublished). CP-chlorpyrifos, DW-distilled water, GW-ground water.

composite was prepared by chemical reduction and they observed that, compared to bare magnetite particles, the hybrids show a high binding capacity for As(III) and As(V). The composites had an added advantage that, they being superparamagnetic at room temperature, can be separated by an external magnetic field after the removal process. A versatile strategy to synthesize various metal/metal oxide graphene composite at room temperature and the utility of these composites for the removal of heavy metals were demonstrated by Sreepasad *et al.*<sup>80</sup> They also devised a green strategy to immobilize these composites onto cheap substrate like sand for easy post treatment handling (Fig. 13). They used an abundant and environmental friendly biopolymer, chitosan for the immobilization, thus avoiding harsh reactants and reaction conditions. The composites showed enhanced removal efficiency compared to some common adsorbents used pointing to their practical utility. Similarly, Gao *et al.* devised a strategy to anchor graphene on sand particles to create an adsorbent for water purification.<sup>81</sup> However, the methodology used diazonium chemistry to functionalize GO and used heat treatment for the immobilization. The use of high energy processes and the use of toxic materials can hinder the use of such systems in high end applications such as water purification.

Koo *et al.* recently reported a graphene based multifunctional iron oxide sheets where needlelike iron oxide (IO) nanoparticles were grown on graphene sheets to have tunable properties.<sup>82</sup> They prepared a paper-like material from the composite which showed extraordinary removal capacity and fast adsorption rates for As<sup>V</sup> and Cr<sup>VI</sup> ions in water. The removal capacities were found to be 218 and 190 mg g<sup>-1</sup> for As<sup>V</sup> and Cr<sup>VI</sup>, respectively. Porous GO/chitosan (PGOC) materials were prepared by a unidirectional freeze-drying method by He *et al.*<sup>83</sup> The metal ion absorption capacity of this composite was investigated. They found a saturated adsorption capacity of Pb<sup>2+</sup> increased about 31%, up to when 5 wt% GO was incorporated in the composite. The maximum capacity obtained was 99 mg/g.

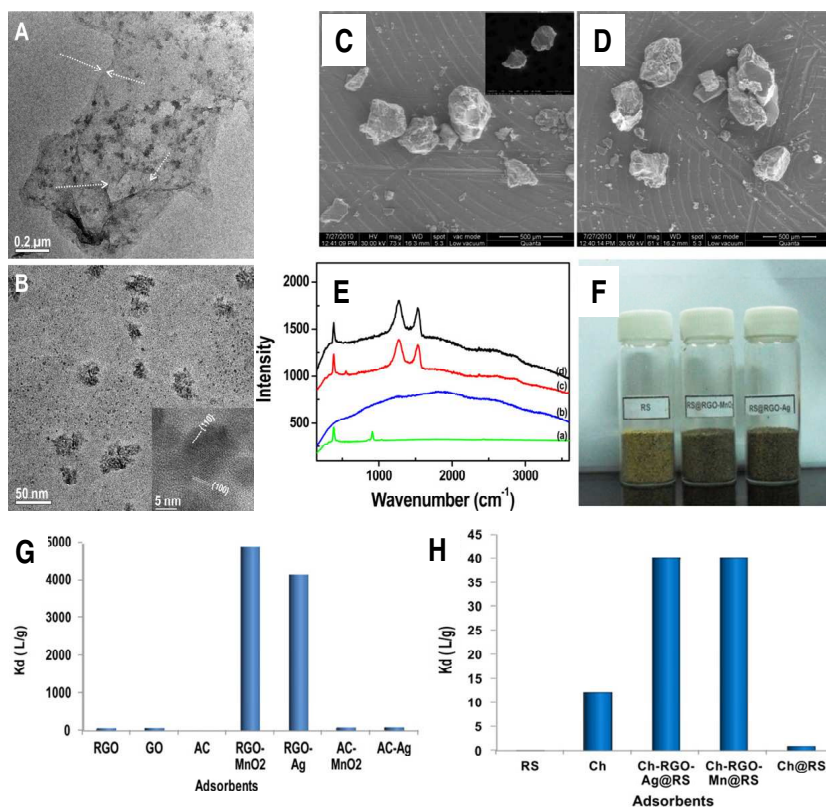


Fig. 13. (A) and (B) TEM images of RGO-MnO<sub>2</sub> (0.05mM) at various magnifications. SEM images of (C) Ch-RGO-Ag@RS, (D) Ch-RGO-MnO<sub>2</sub>@RS; inset in 'C' shows a SEM image of bare sand particles, (E) Raman spectrum of (a) RS, (b) Ch, (c) Ch-RGO-MnO<sub>2</sub>@RS, and (d) Ch-RGO-Ag@RS, (F) photograph of RS, Ch-RGO-MnO<sub>2</sub>@RS and Ch-RGO-Ag@RS (G) unsupported RGO composites with other adsorbents (H) supported RGO composite with RS, Ch, Ch@RS. *Source:* Adapted from Sreepasad *et al.* (2011).

A polypyrrole-RGO composite, which is highly selective towards the adsorption of Hg<sup>2+</sup> was also reported recently.<sup>84</sup> The synthesis was done through the chemical exfoliation of graphite to GO and the subsequent reduction to RGO in the presence of polypyrrole (PPy). PPy-RGO composite having 15 wt% GO loading exhibited highly selective and enhanced absorption of Hg<sup>2+</sup>. A high adsorption efficacy up to 980 mg g<sup>-1</sup> and an extremely high desorption capacity of up to 92.3%, showed by the composite pointed towards the repeatable applicability of the proposed composite. Zhang *et al.* also devised a strategy to make GO-ferric hydroxide composites which can be efficient for the removal of arsenate from drinking water.<sup>85</sup> The composite include GO cross linked with ferric hydroxide where, the amorphous ferric hydroxide was found to be homogenously impregnated onto GO. More than 95% arsenate removal was obtained for the water with arsenate concentration at 51.14 ppm, implying an absorption capacity of 23.78 mg arsenate/g of composite.

They also pointed out that the adsorption can be effective in a wide range of pH from 4 to 9. However, a decreased adsorption efficacy was exhibited for pH greater than 8.<sup>85</sup> A graphene-based magnetic nanocomposite for the removal of an organic dye, fuchsine from aqueous solution was reported by Wang *et al.*<sup>86</sup> They prepared RGO-Fe<sub>3</sub>O<sub>4</sub> composite by the *in situ* chemical coprecipitation of Fe<sup>2+</sup> and Fe<sup>3+</sup> in alkaline solution in the presence of RGO. The study included the investigation of adsorption kinetics, capacity of the adsorbent, the effect of the adsorbent dosage and solution pH on the removal efficiency of fuchsine.

Graphene/magnetite composite synthesized by solvothermal methods were used for the removal of methylene blue from aqueous solutions.<sup>87</sup> Here, they achieved *in situ* conversion of FeCl<sub>3</sub> to Fe<sub>3</sub>O<sub>4</sub> and simultaneous reduction of GO to RGO in ethylene glycol solution. This composite showed extraordinary adsorption capacity and fast adsorption rates for removal of MB. A similar method for the preparation of RGO-Fe<sub>3</sub>O<sub>4</sub> was reported by Sun *et al.* as well.<sup>88</sup> They observed the composite to be excellent for the removal of rhodamine B (91%) and malachite green (over 94%). They also found that the removal is strongly dependent on both the loading of Fe<sub>3</sub>O<sub>4</sub> and the pH value. They demonstrated that the composite can be applied in real water systems including industrial waste water and lake water. Using chemical deposition method, Mg(OH)<sub>2</sub>-RGO composite (MGC) was synthesized by Li *et al.*<sup>89</sup> The formed composite had a mesoporous structure and was found to be efficient in removing MB from water. The Mg(OH)<sub>2</sub> nanostructures formed were highly dispersed on the RGO sheet and had high surface area. It also aided in increasing the pore volume, and to create a uniform pore width distribution. A similar Cu<sub>2</sub>O-RGO composite (CGC) has also been reported.<sup>90</sup> The composite was projected for removal of dye from water and in supercapacitors. CGC exhibited a high adsorption capacity for rhodamine B (RhB), and MB. Using these composites, a reactive filtration film was assembled and was applied to remove dye from waste water.

#### 4. Application of Graphene in Biology Other than Sensing

The discovery of ways to make graphene in bulk quantities, especially the chemical ways of preparing GO and RGO by the oxidation of graphite opened up the application of these materials in various fields. Biology being a key field where nanomaterials find tremendous application possibility, graphenic materials have been drawing interest in this area as well. Chemically prepared graphene has rich abundance of functional groups such as hydroxyl, carboxylic acid and other reactive groups which are amenable to ligand conjugation, cross-linking and other modifications, rendering GO/RGO tailored for a range of biomedical and other applications. Again, the abundance of hydrophilic functionalities renders them good biocompatibility as well. Here, a brief overview of efforts taken up to use graphene in biology is presented. The biocompatibility of graphene was investigated recently. Graphene based biocompatible paper was prepared and its biocompatibility was demonstrated by

culturing mouse fibroblast cell line (L-929).<sup>91</sup> The cell lines were found to adhere to and proliferate on graphene papers. A sub-confluent layer of metabolically active cells were formed within 48 h of culture time. Agarwal *et al.* tested biocompatibility of RGO with rat pheochromocytoma (neuroendocrine cell, PC12) cells, human oligodendroglia (HOG) cells and human fetal osteoblast (hFOB) cells.<sup>92</sup> Many efforts have been undertaken to incorporate biomaterials,<sup>93,94</sup> such as DNA,<sup>19,95,96</sup> protein<sup>97–99</sup> to graphene.

Most of these were aimed at developing FETs or sensing. Some of these efforts have been mentioned in earlier sections. GO/RGO has tremendous ability to adsorb DNA. It can quench the luminescence from biomolecules, and can protect them from enzyme cleavage as well. Hence, GO and RGO are being utilized frequently in biotechnology and several investigations, including drug delivery, cellular imaging, real-time monitoring, cell imaging, *in vivo* targeting of ATP and *in situ* localization of mRNA. In this section, we review some of applications of graphene and graphene-based nanomaterials in live cells.

The ability of graphene to protect DNA from cleavage during cellular delivery was demonstrated by Lu *et al.* Molecular beacons (MBs) were used as oligonucleotide probes in combination with GO sheets to deliver DNA to HeLa cells, where graphene served as the protective covering for the DNA.<sup>100</sup> Wang *et al.* in 2010 designed an aptamer–carboxyfluorescein/GO nanosheet (aptamer–FAM/GO-nS) complex for *in situ* molecular analysis of ATP in JB6 Cl 41-5a mouse epithelial cells.<sup>101</sup> The formed composite with the aid of a wide-field fluorescence microscope, served as a real-time sensing platform. GO/RGO was used for drug delivery vehicle as well. Liu *et al.* in 2008 was the first one to use graphene as a cargo for the delivery of water-soluble cancer drugs.<sup>102</sup> Functionalization of GO with polyethylene glycol (PEG) to ensure better solubility of GO in aqueous solutions, as well as stability in physiological solutions. The drug delivery capacity was enhanced by anchoring SN<sub>38</sub> (a water-insoluble aromatic compound), and the composite exhibited high efficiency in carrying cancer drug to HCT-116 human colon cancer cells. Later, Zahng *et al.* found that GO conjugated with folic acid (FA) can enhance the loading efficiency and targeting ability of anticancer drugs.<sup>103</sup> They investigated two anticancer drugs, doxorubicin and CPT-11 onto the FA-conjugated GO (FA-GO) and found that the two anticancer drugs show specific targeting to MCF-7 human breast cancer cells. Recently Yang *et al.* utilized the strong optical absorbance of PEGylated GO in the near-infrared region to develop ultra-high *in vivo* tumor uptake of anticancer drugs, and to use them for photothermal therapy of cancer.<sup>104</sup> Some graphene based FETs for living cell detection has also been documented. A graphene-based FET was used to investigate electrogenic cells by Cohen–Karni *et al.*<sup>105</sup> They obtained FET conductance signals recorded from beating chicken embryonic cardiomyocytes yielding well-defined extracellular signals. He *et al.* used a graphene-based FET as a biosensor to detect hormonal catecholamine molecules in neuroendocrine PC12 rat adrenal medulla cells.<sup>106</sup> In

this study, a patterned GO film-based FET was constructed and it was developed into a label-free and real-time monitoring FET for catecholamine secretion from living cells.

## 5. Conclusions and Outlook

The fascinating properties of graphene, with respect to structures that can be modulated and surfaces that can be modified, offers some important advantages for novel applications in biotechnology and environmental science, especially in the areas of biosensors and medicine, contaminant sensing and remediation. However, the use of graphene in this field is in its infancy and many challenges remain. This review illustrated the potential of graphene or graphene based materials for applications other than catalytic or electronic processes. Recently, several efforts have been dedicated to use the extraordinary properties of graphene in fields such as sensing, biotechnology and environmental remediation. Utilizing the high surface area and the presence of a variety of functional groups, the properties of graphene can be tuned for various applications. Functionalization of graphene surface with specific target molecules can develop novel targeted sensors. By incorporating different materials, graphene can be used for FET based, voltammetric, FRET based or SERS based sensing applications. However, challenges still exist in this area. For example, even though pristine graphene (graphene obtained from physical exfoliation) has tremendous capability for FRET based application, it is highly hydrophobic which limits the application. Similarly, GO is highly hydrophilic but, its electrical conductivity is comparatively very low. Likewise, some challenges exist in the bulk production of soluble, well-defined graphene or graphene derivatives. Cytotoxicity, the cellular uptake mechanism, and the intracellular metabolic pathway of graphene and its derivatives are not known in detail. Although the initial results are promising, a thorough knowledge about these are necessary before using these systems for *in vivo* applications.

However, an area in which graphene or chemically synthesized GO/RGO is believed to make immediate impact is in water decontamination. This review clearly demonstrated the usefulness of graphenic materials in this field. Various strategies such as photocatalytic degradation, capacitive deionization, membrane separation and adsorption based removal can be used for this cause. Graphene-based materials were found to be useful in all these fields. Among these technologies, adsorption is proved to be most efficient and economically viable, especially for removing pollutants from dilute solutions. Due to the large surface area and the abundance of functional groups, GO/RGO is the best suitable candidate for low cost-high efficiency adsorbent, which is the need of the hour. The separation of graphenic adsorbent from the solution after remediation process was a challenge until recently. Researchers have found novel techniques to overcome this difficulty as well. Hence, it is believed that over the next few years, water treatment will emerge as one of the chief areas of application for graphene, especially GO/RGO.

## Acknowledgment

The authors thank the Department of Science and Technology, Government of India for supporting their research program on nanomaterials.

## References

1. T. Pradeep and Anshup, *Thin Solid Films* **517**, 6441 (2009).
2. F. Schedin *et al.*, *Nat. Mater.* **6**, 652 (2007).
3. H. Vedala *et al.*, *Nano Lett.* **11**, 2342 (2011).
4. T. Zhang *et al.*, *Nano Lett.* **10**, 4738 (2010).
5. G. Lu *et al.*, *Chem. Commun.* **47**, 7761 (2011).
6. S. Liu *et al.*, *Biosens. Bioelectron.* **26**, 4491 (2011).
7. Y. Wang *et al.*, *ACS Nano* **4**, 1790 (2010).
8. B. G. Choi *et al.*, *ACS Nano* **4**, 2910 (2010).
9. C. Shan *et al.*, *Langmuir* **25**, 12030 (2009).
10. H. Du *et al.*, *J. Electroanal. Chem.* **650**, 209 (2011).
11. J. Gong *et al.*, *Sens. Actuators B: Chem.* **150**, 491 (2010).
12. J. Li *et al.*, *Electrochem. Commun.* **11**, 1085 (2009).
13. Y. Yao *et al.*, *Appl. Surf. Sci.* **257**, 7778 (2011).
14. Z. Jiang *et al.*, *Chem. Commun.* **47**, 6350 (2011).
15. S. Deng *et al.*, *Biosens. Bioelectron.* **26**, 4552 (2011).
16. X. Liu *et al.*, *ACS Appl. Mater. Interfaces* Article ASAP (DOI:10.1021/am200737b) (2011).
17. W. Ren, Y. Fang and E. Wang, *ACS Nano* **5**, 6425 (2011).
18. C.-H. Lu *et al.*, *Angewandte Chemie Int. Ed.* **48**, 4785 (2009).
19. N. Mohanty and V. Berry, *Nano Lett.* **8**, 4469 (2008).
20. Y. Ohno, K. Maehashi and K. Matsumoto, *Biosens. Bioelectron.* **26**, 1727 (2010).
21. H. Jang *et al.*, *Angewandte Chemie Int. Ed.* **49**, 5703 (2010).
22. S. He *et al.*, *Adv. Funct. Mater.* **20**, 453 (2010).
23. H. Dong *et al.*, *Anal. Chem.* **82**, 5511 (2010).
24. C.-H. Lu *et al.*, *Chem. – A Euro. J.* **16**, 4889 (2010).
25. B. G. Choi *et al.*, *Nanoscale* **2**, 2692 (2010).
26. Y. Wen *et al.*, *Chem. Commun.* **46**, 2596 (2010).
27. H. Chang *et al.*, *Anal. Chem.* **82**, 2341 (2010).
28. C. Zhang *et al.*, *Angewandte Chemie Int. Ed.* **50**, 6851 (2011).
29. Y. Xu, A. Malkovskiy and Y. Pang, *Chem. Commun.* **47**, 6662 (2011).
30. C. Wu *et al.*, *Analyst* **136**, 2106 (2011).
31. H. Wang *et al.*, *Angewandte Chemie Int. Ed.* **50**, 7065 (2011).
32. W. T. Huang *et al.*, *Chem. Commun.* **47**, 7800 (2011).
33. X.-H. Zhao *et al.*, *Anal. Chem.* **83**, 5062 (211).
34. Z. Xiong *et al.*, *Chem. Commun.* **46**, 6099 (2010).
35. M. Zhu, P. Chen and M. Liu, *ACS Nano* **5**, 4529 (2011).
36. O. Akhavan and E. Ghaderi, *J. Phys. Chem. C* **113**, 20214 (2009).
37. J. Liu *et al.*, *Adv. Funct. Mater.* **20**, 4175 (2010).
38. C. Chen *et al.*, *ACS Nano* **4**, 6425 (2010).
39. Y. Zhang *et al.*, *ACS Nano* **4**, 7303 (2010).
40. Q. Zhang *et al.*, *Chin. Sci. Bull.* **56**, 331 (2011).
41. B. Jiang *et al.*, *Chem. Eur. J.* **17**, 8379 (2011).
42. H. Zhang *et al.*, *ACS Nano* **4**, 380 (2010).
43. Y. Liang *et al.*, *Nano Res.* **3**, 701 (2010).

44. G. Jiang *et al.*, *Carbon* **49**, 2693 (2011).
45. J. Guo *et al.*, *Ultras. Sonochem.* **18**, 1082 (2011).
46. T.-D. Nguyen-Phan *et al.*, *Chem. Eng. J.* **170**, 226 (2011).
47. B. Li and H. Cao, *J. Mater. Chem.* **21**, 3346 (2011).
48. S. Chen *et al.*, *J. Solid State Chem.* **183**, 2552 (2010).
49. F. Zhang *et al.*, *J. Phys. Chem. C* **114**, 8469 (2010).
50. X. Cai *et al.*, *Langmuir* **27**, 7828 (2011).
51. J. Ma *et al.*, *J. Mater. Chem.* **21**, 3350 (2011).
52. Q. Bao, D. Zhang and P. Qi, *J. Colloid Interface Sci.* **360**, 463 (2011).
53. L. Liu *et al.*, *New Chem.* **35**, 1418 (2011).
54. T. S. Sreepasad *et al.*, *ACS Appl. Mater. Interfaces* **3**, 2643 (2011).
55. H. Li *et al.*, *J. Mater. Chem.* **19**, 6773 (2009).
56. H. Li *et al.*, *Sep. Purif. Technol.* **75**, 8 (2010).
57. H. Li *et al.*, *Environ. Sci. Technol.* **44**, 8692 (2010).
58. H. Li *et al.*, *J. Electroanal. Chem.* **653**, 40 (2011).
59. A. Hashimoto *et al.*, *Nature* **430**, 870 (2004).
60. M. M. Lucchese *et al.*, *Carbon* **48**, 1592 (2010).
61. N. Inui *et al.*, *Appl. Phys. A: Mater. Sci. Process.* **98**, 787 (2010).
62. D. Wei *et al.*, *Nano Lett.* **9**, 1752 (2009).
63. K. Sint, B. Wang and P. Krail, *J. Am. Chem. Soc.* **131**, 9600 (2009).
64. M. Zabihi, A. Ahmadpour and A. H. Asl, *J. Hazard. Mater.* **167**, 230 (2009).
65. D. Ayhan, *J. Hazardous Mater.* **167**, 1 (2009).
66. S. M. Maliyekkal, K. P. Lisha and T. Pradeep, *J. Hazard. Mater.* **181**, 986 (2010).
67. P. A. Denis and F. Iribarne, *J. Mole Struct. Theochem* **957**, 114 (2010).
68. X. Deng *et al.*, *J. Hazard. Mater.* **183**, 923 (2010).
69. S.-T. Yang *et al.*, *J. Colloid Interface Sci.* **351**, 122 (2010).
70. Q. Liu *et al.*, *Angewandte Chemie Int. Ed.* **50**, 5913 (2011).
71. T. S. Sreepasad, S. S. Gupta, S. M. Maliyekkal and T. Pradeep, Unpublished (2011).
72. G. K. Ramesha *et al.*, *J. Colloid Interface Sci.* **361**, 270 (2011).
73. S.-T. Yang *et al.*, *J. Colloid Interface Sci.* **359**, 24 (2011).
74. W. Zhang *et al.*, *Bull. Environ. Contam. Toxicol.* **87**, 86 (2011).
75. G. Zhao *et al.*, *Adv. Mater.* **23**, 3959 (2011).
76. Y. Li *et al.*, *J. Colloid Interface Sci.* **363**, 348 (2011).
77. K. Mishra and S. Ramaprabhu, *Desalination* In Press, Corrected Proof (doi:10.1016/j.desal.2011.01.038) (2011).
78. S. M. Maliyekkal, T. S. Sreepasad, K. Deepti and T. Pradeep, T. Unpublished.
79. V. Chandra *et al.*, *ACS Nano* **4**, 3979 (2010).
80. T. S. Sreepasad *et al.*, *J. Hazard. Mater.* **186**, 921 (2011).
81. W. Gao *et al.*, *ACS Appl. Mater. Interfaces* **3**, 1821 (2011).
82. H. Y. Koo *et al.*, *Chem. Eur. J.* **17**, 1214 (2011).
83. Y. Q. He, N. N. Zhang and X. D. Wang, *Chin. Chem. Lett.* **22**, 859 (2011).
84. V. Chandra and K. S. Kim, *Chem. Commun.* **47**, 3942 (2011).
85. K. Zhang *et al.*, *J. Hazard. Mater.* **182**, 162 (2010).
86. C. Wang *et al.*, *Chem. Eng. J.* **173**, 92 (2011).
87. L. Ai, C. Zhang and Z. Chen, *J. Hazard. Mater.* **192**, 1515 (2011).
88. H. Sun, L. Cao and L. Lu, *Nano Res.* **4**, 550 (2011).
89. B. Li, H. Cao and G. Yin, *J. Mater. Chem.* **21**, 13765 (2011).
90. B. Li *et al.*, *J. Mater. Chem.* **21**, 10645 (2011).
91. H. Chen *et al.*, *Adv. Mater.* **20**, 3557 (2008).
92. S. Agarwal *et al.*, *Langmuir* **26**, 2244 (2010).

93. T. H. Han *et al.*, *Adv. Mater.* **22**, 2060 (2010).
94. Q. Yang *et al.*, *J. Phys. Chem. C* **114**, 3811 (2010).
95. L. A. L. Tang, J. Wang and K. P. Loh, *J. Am. Chem. Soc.* **132**, 10976 (2010).
96. J. Liu *et al.*, *J. Mater. Chem.* **20**, 900 (2010).
97. J. Zhang *et al.*, *Langmuir* **26**, 6083 (2010).
98. P. Laaksonen *et al.*, *Angewandte Chemie Int. Ed.* **49**, 4946 (2010).
99. J. Liu *et al.*, *J. Am. Chem. Soc.* **132**, 7279 (2010).
100. C.-H. Lu *et al.*, *Chem. Commun.* **46**, 3116 (2010).
101. Y. Wang *et al.*, *J. Am. Chem. Soc.* **132**, 9274 (2010).
102. Z. Liu *et al.*, *J. Am. Chem. Soc.* **130**, 10876 (2008).
103. L. Zhang *et al.*, *Small* **6**, 537 (2010).
104. K. Yang *et al.*, *Nano Lett.* **10**, 3318 (2010).
105. T. Cohen-Karni *et al.*, *Nano Lett.* **10**, 1098 (2010).
106. Q. He *et al.*, *ACS Nano* **4**, 3201 (2010).